energies

MDPI

Article

Impact of Shading Effect from Nearby Buildings on Energy Demand and Load Calculations for Historic City Centres in Central Europe

Agnieszka Sadłowska-Sałęga * and Krzysztof Wąs

Department of Rural Building, Faculty of Environmental Engineering and Geodesy, University of Agriculture in Krakow, 30-059 Krakow, Poland; krzysztof.was@urk.edu.pl
* Correspondence: agnieszka.sadlowska@urk.edu.pl

Abstract: EU legislation requires introducing a variety of measures to reduce energy consumption. Energy use decrease should be achieved through thermal retrofitting of the least energy-efficient buildings. In the case of cities like Kraków, this means the need to modernize (retrofitting as well as the incorporation of modern HVAC systems) historical buildings. Furthermore, urban morphology is an influencing factor with regards to the energy performance of buildings and therefore of cities (since the influence of shading from nearby buildings cannot be ignored). The paper presents the results of a study on the impact of shading on energy demand for heating and cooling in the historic centre of Krakow. A comparative analysis of the simulation calculation results was performed using the statistical climate as a boundary condition. In the case of a typical five-floor residential tenement house from the turn of the 20th century, an 8% increase in energy demand for heating and a 50% reduction in energy demand for cooling were estimated. As the analysis of the results shows, taking into account the shading from nearby buildings may be crucial for optimizing the volume (power of devices, diameters of ducts and pipes) of the HVAC installation.

Keywords: energy-efficient HVAC systems; historical buildings; retrofitting; shading effect; energy demand

Citation: Sadłowska-Sałęga, A.; Wąs, K. Impact of Shading Effect from Nearby Buildings on Energy Demand and Load Calculations for Historic City Centres in Central Europe. *Energies* **2024**, *17*, 6400. https://doi.org/10.3390/en17246400

Academic Editors: Joanna Ferdyn-Grygierek, Krzysztof Grygierek and Agnes Psikuta

Received: 19 November 2024
Revised: 14 December 2024
Accepted: 17 December 2024
Published: 19 December 2024

1. Introduction

1.1. Literature Review

Urban morphology has been pointed out as one of the influencing factors with regards to the energy performance of cities. Studies show that in Central European cities, there are characteristic patterns illustrating strong investment in city centres and low diversity of land cover and use in historic city cores [1]. At the same time, it has been shown that in Poland, after EU accession, there have been more rapid changes in land use than in other Central European countries [2]. Additionally, in functional urban areas of Poland, there is an encroachment of urbanized areas into suburban areas, and thus an increase in the diversity of land cover and use in the access zones of cities [3]. As a result, so-called heat islands occur due to the uniformity of development and the disappearance of natural areas. The formation of urban heat islands, together with the ongoing climate change, has led to changes in energy demand for urbanized areas. For example, climate change in Europe is causing a significant increase in demand for cooling—even in regions (such as Poland) where cooling of buildings during the summer has so far been uncommon. This means an increased installation rate of air conditioning systems in buildings. European Union legislation requires implementing measures to reduce energy consumption for heating and cooling. The EU aims to reduce residential energy consumption by 16% by 2030 and 20–22% by 2035. National measures will have to ensure that at least 55% of the decrease in the average primary energy use is achieved through the renovation of the least energy-efficient buildings focusing on the thermal retrofitting of them [4]. In the case of cities like Kraków,

this task is difficult to accomplish. This is because a large part of the city is listed for special protection as national heritage (a significant number of buildings in the city centre were built at the turn of the 20th century), whilst the medieval the old town was among the first sites chosen for UNESCO's original World Heritage List. The condition of the load-bearing structures of the buildings is usually satisfactory. However, secondary structures and heating systems are outdated and inefficient.

Restoration of historical buildings is one of the important trends of cultural heritage and has been studied and discussed for years [5–7]. Many new technologies have been developed to this day, but the retrofitting process has never been a simple undertaking owing to historical preservation codes, restrictions created by the existing building structure, and the threat that the latter poses to historical integrity [8,9]. In many cases, in residential buildings, thermal modernization comes down to replacing windows with more energy-efficient ones and insulation of the ceiling below an unheated attic. Incorporating modern HVAC systems into historical buildings is not a straightforward task as it is accompanied by a number of challenges [8]:

- old structures are made of different materials from those used in today's construction practices, which makes it difficult to incorporate a new system without causing harm to the rest of the structure;
- the thickness and the materials used for constructing partitions pose a challenge when trying to install ducts or piping fixtures;
- any external changes, such as the installation of vents, thermostats or other HVAC devices, have to be made in a way that will not alter the overall character of the building).

For this reason, the correct dimensioning of HVAC installation is crucial.

Heating and cooling load calculations are carried out to estimate the required capacity of the heating and cooling systems needed to maintain the required environment in the conditioned space. In most cases, calculations are made on the basis of steady-state methodology [10–12]. In these methods, the shading resulting from the use of shading devices (e.g., blinds) is considered in the cooling load calculations, but the surroundings of the building are not.

The positive effect of shading from nearby buildings on reducing solar gains was already known in ancient times in the Mediterranean basin [13]. In recent years, much attention has also been paid to investigating the influence (positive as well as negative) of shading from nearby buildings on the heating and cooling demand in temperate climates. Assuming that a reduction in the energy consumption of buildings is an effective means to build a low-carbon city, it has become essential for planners and designers to consider buildings as integral elements of the urban environment rather than stand-alone entities. This is related to the rational prediction of regional space cooling/heating loads and the design of distributed energy resource systems [14].

The analysis of the energy performance of buildings in relation to urban and street planning can become a theoretical basis for rational architectural layout and energy consumption reduction [15]. The influence of land development on the formation of the urban climate is expressed by various indicators. For example, the concept of the urban canyon is a model widely used in energy studies [16]. Its geometric layout may be described based on the following:

- its axis orientation;
- its cross-sectional dimensions: width of the street (W) and height of the building (H).

Aspect ratio (W/H) or inverted aspect ratio (H/W) are intuitive ways of characterizing the occlusion of an urban fabric. Canyon morphology has also been described quantifying the total amount of visible sky from a particular point, using other parameters such as the Sky View Factor (SVF) [17,18] or Sky Factor (SF) [19]. The larger the H/W, the smaller the SVF, meaning that the shading effect is stronger, resulting in a decrease in solar radiation reaching the ground and affecting thermal environment of street canyons.

There are also some index parameters that describe the relationship between buildings and the open area in a constant plot. The Floor Area Ratio (*FAR*) is one such parameter, which is the ratio of the built area to the lot area. A larger *FAR* value indicates a greater volume of the building. The Building Coverage Ratio (*BCR*) is the relationship between the ground floor area of enclosed buildings and the area of the land plot. Development scenarios where the *FAR* is same but the *BCR* is different will produce varying types of development, such as low rise or high rise, which can be incorporated into different layouts of buildings [14].

The H/W ratio is associated with thermal comfort in urban street canyons [20] (in some cases, with a different H/W the difference in dry-bulb temperature can reach 10 °C [21]), which affects the energy demand of buildings. Huang et al. [22], Oke [23] and Arnfield [24] proved in their works that H/W is a significant parameter influencing how much solar radiation reaches buildings. For example, for Hong Kong, the increase in energy demand due to shading from nearby buildings was determined to be 2% [25]. Other studies show that reductions in space cooling reach up to 30% [25,26]. Research using a hypothetical nine-building block that contained a three-storey commercial reference building [27] in eight cities in the U.S. indicated that the building's energy consumption can increase by 60.4% compared with a building without shading.

Over the past decades, detailed individual Building Energy Models (BEMs) have become established modes of analysis for building designers and energy policy makers. More recently, these models have evolved into so-called Urban Building Energy Models (UBEMs) [28,29] taking into account the energy performance of neighbourhoods, i.e., several dozens to thousands of buildings. This term is attributed explicitly to bottom–up (intended to focus on individual buildings [30]) engineering models. In the case of large-scale models, even a slight increase in resolution for one or more aspects can lead to a noticeable growth in the computational burden due to the issue of dimensionality [30]. Considering that the modernization of historic buildings is essentially a case study, the solution may be to use BEMs that take into account the building's immediate surroundings. Modern calculation tools such as EnergyPlus or WUFI®plus allow for the accurate assessment of heat gains and losses in buildings. They also have the ability to perform calculations that take into account shading from nearby buildings [26,31].

There are different ways of taking the shading into account. The most common is the adaption of radiation gains by reduced absorption and emission coefficients. Another way is calculating the radiation load by determining the position and size of the shading object in the field of view of the receiving surface [32].

1.2. Aim of the Study

Climate is a major factor that affects shading, apart from the index parameters and building layouts [14,33]. Most of the research in this field concerns warm climates or areas with modern buildings (e.g., [34]). Therefore, the aim of the study was to investigate the influence of shading from nearby buildings on the energy demand for heating and cooling as well as heating and cooling loads (for the entire building and individual floors of the building treated as separate calculation zones), in a temperate climate of Central Europe in the case of historical city centres, using Kraków as an example.

2. Materials and Methods

Calculations were performed using WUFI®plus software (ver. 3.5), enabling comprehensive thermal and moisture analysis of entire buildings, taking into account heat exchange with the ground [35]. As studies comparing contemporary BEMs (such as EnergyPlus, WUFI®Plus or ESP-r) show, there are no significant differences in their general accuracy [36,37]. However, the studies described in [38] have shown that in terms of goodness of fit, the WUFI®Plus model attains a significantly higher temperature fit as well as a higher water vapour pressure fit when compared to the EnergyPlus model. WUFI®Plus is the most complete heat and moisture simulation tool in the WUFI software family. It has

been tested many times for use in calculations of historical buildings (including many times by the authors of this study [39–44]). It is a recognized tool used in so-called preventive conservation and collection care [39,44,45]. One of its advantages, in the case of calculations for historical buildings, is the extensive database of historical building materials.

The analyses carried out according to the block chart (Figure 1) include comparison of the results of energy demand calculations in transient conditions with and without taking into account the shading from nearby buildings, supplemented by a shortened comparison of the results of the heating and cooling loads in transient conditions with steady-state calculation (without shading from nearby buildings).

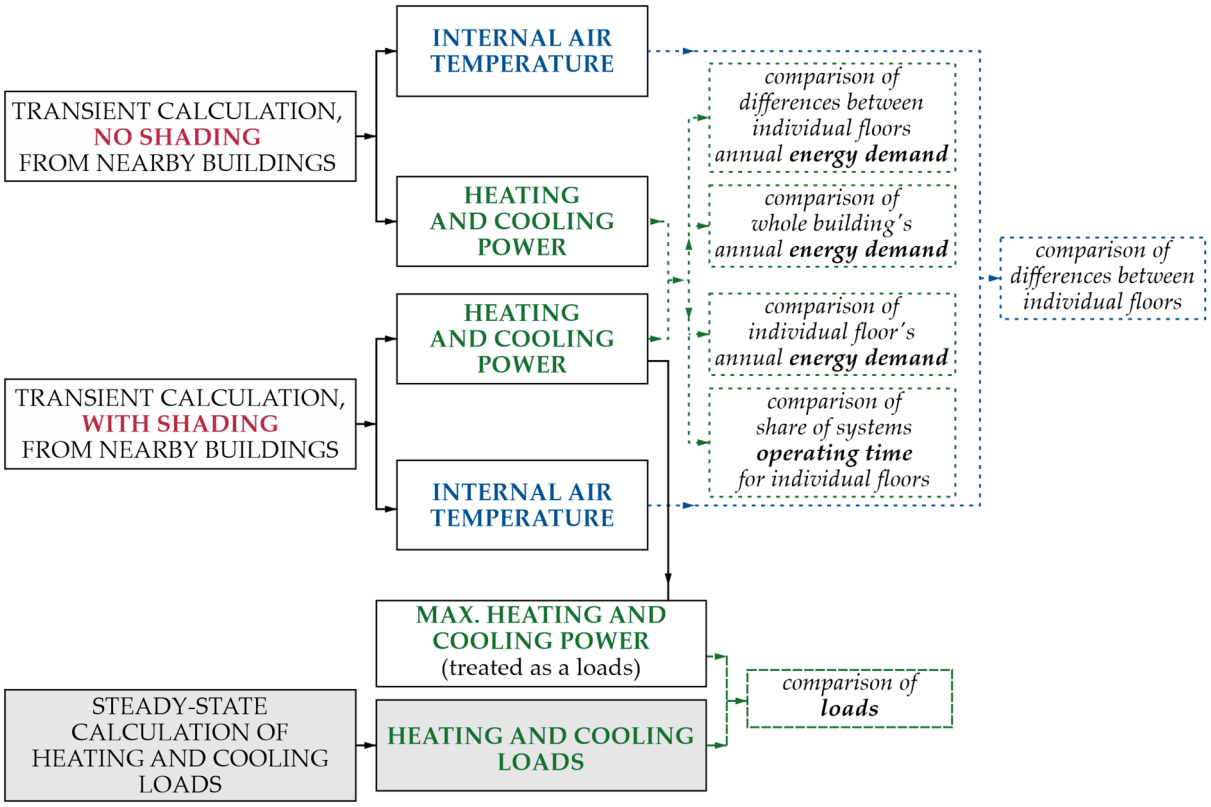

Figure 1. The block chart of conducted analyses.

For every simulation time step, the shading of the building components and windows is calculated depending on solar position and the building's visualized 3D geometry [46].

2.1. Case Study

The paper is based on the analysis of a generic multi-family residential tenement house representative of the old, historical centre of Kraków. Tenement houses in this part of the city are most often connected to each other in a closed quadrangle block, which has a large courtyard inside (Figure 2). They have a masonry structure and are most often made of full ceramic bricks. The thickness of the structure usually exceeds 40 cm (in some cases can even reach up to 100 cm). The ceilings are made using various technologies, including wooden structures, structures with steel beams or monolithic structures. The buildings usually have 3 to 5 floors above ground level.

Windows in these types of buildings are box structures with two layers of glazing, which, over the last two decades, have been gradually replaced with double- or triple-glazed composite structures as a result of thermal modernization activities. Also, ceilings below unheated attics or above unheated basements as well as the roof slopes have been additionally insulated to reduce energy losses. On the other hand, external walls very often

cannot be insulated from the outside, due to conservation restrictions, and only insulation from the inside is allowed, which is rarely implemented by owners.

(a) (b)

Figure 2. View of the streets of Kraków (reproduced from [47]) (**a**) and typical layout of Kraków's buildings in its historic centre (**b**).

The distance between individual blocks of tenement houses in the analysed area ranges from 16 to 20 m, excluding larger road arteries. The discussed arrangement is presented in the layout in Figure 2.

2.2. Three-Dimensional Model of the Building

For the analyses of heat gains and losses, a generic building was created along with a fragment of a typical urban layout:

1. A two-dimensional generic urban layout characteristic of Kraków's development at the turn of the 20th century was prepared based on publicly available maps (Figure 3a).
2. On this basis, a three-dimensional model of the analysed building and the surrounding buildings was modelled using the SketchUp tool (Figure 3b).
3. The last stage was the implementation of the developed model in WUFI®Plus, a tool for dynamic thermal and moisture analysis (Figure 3c).

The final building model is presented in Figure 4. It should be noted that the building model was created in two variants. Variant 1 does not take into account the nearby buildings (Figure 4a), and therefore does not take into account the shading generated by these buildings. Variant 2 takes into consideration the nearby buildings (Figure 4b). The modelled building has 5 floors above ground with a room height of 3.7 m. Each floor has an area of 672 m^2, which translates into a total building area of 3360 m^2. The tenement house has an L-shape with dimensions of 27 × 36 m and its height is 23 m (Figure 5). The building is located in the south-western corner of the tenement house block, among other buildings of the same height.

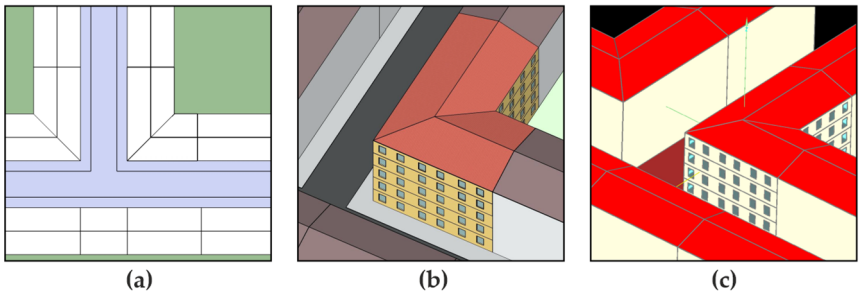

(a) (b) (c)

Figure 3. The process of creating a building model: a two-dimensional generic urban layout (**a**), 3D model in SketchUp (**b**) and 3D model in WUFI®plus (**c**).

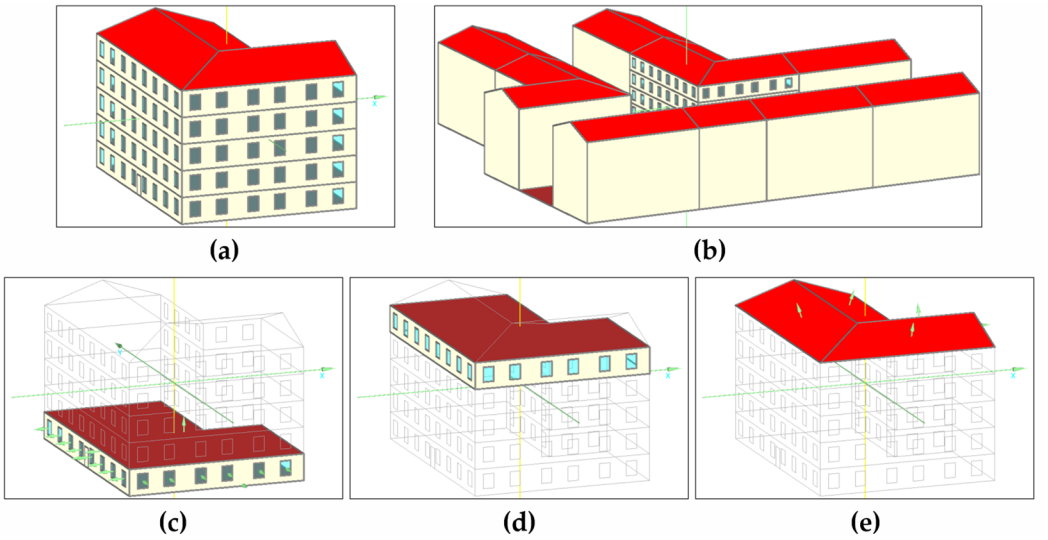

Figure 4. 3D building model in WUFI®plus: without nearby buildings (**a**) and with them (**b**), as well as division of the building into zones: first floor (**c**), fifth floor (**d**) and unused attic (**e**).

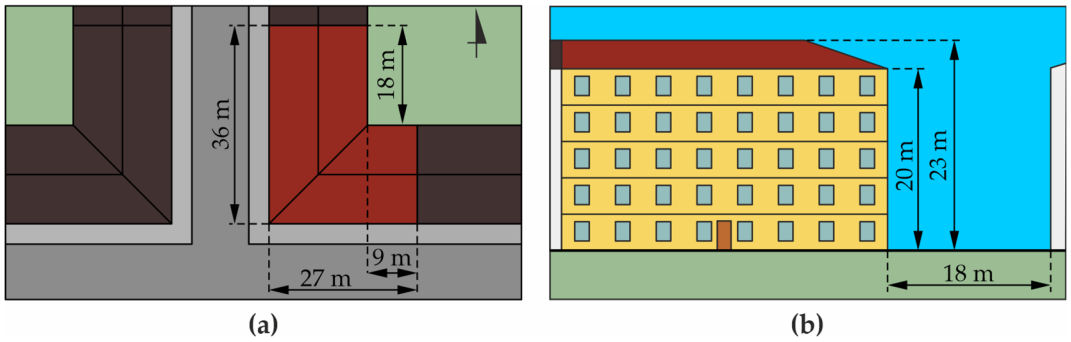

Figure 5. Building dimensions: length and width (**a**) and height (**b**).

The building was divided into a total of seven simulation zones (Figure 4c–e). Each of the five floors was considered a separate zone: the five inhabited floors, unused attic. Adjacent buildings were combined into one zone. Each floor was divided into 5 apartments and a staircase. Internal partitions were included in the model as so-called non-visualized components. As a result, they affected the building's accumulation capacity.

All partitions, except ceilings and floors, were made with the use of masonry technology. The thickness of the brick wall was assumed to be 48 cm for load-bearing walls and 16 cm for partition walls. Additionally, a 1 cm layer of plaster was assumed on both sides of each of the walls. The ceilings were assumed to be of reinforced concrete construction with a thickness of 30 cm. In the case of the unheated attic, additional insulation was installed with a layer of 10 cm thick polystyrene. The *U*-factor for the external walls is 1.005 $W \cdot m^{-2} \cdot K^{-1}$. The double-glazed windows have dimensions of 1.6 × 2.2 m. Facing the street, there are 8 windows on the western elevation and 6 on the southern one. Facing the courtyard, there are 2 windows on the northern elevation and 4 on the eastern one. The *U*-factor for the windows is 1.6 $W \cdot m^{-2} \cdot K^{-1}$ and the solar heat gain coefficient (*SHGC*) is 0.7. The basic parameters of the partitions are presented in Tables 1–5.

Only shading from nearby buildings is included in the calculations. The model does not include any shading devices or elements. Due to the historic nature of the buildings in the center of Kraków and the conservation care, it is not possible to install shading elements on the outside of the building.

Table 1. Partition design parameters of the load-bearing walls.

Layers	Thickness [m]	Thermal Conductivity [W·m^{-1}·K^{-1}]	*U*-Value [W·m^{-2}·K^{-1}]
Plaster	0.010	0.80	1005
Solid brick	0.480	0.60	
Plaster	0.010	0.80	

Table 2. Partition design parameters of the partition walls.

Layers	Thickness [m]	Thermal Conductivity [W·m^{-1}·K^{-1}]	*U*-Value [W·m^{-2}·K^{-1}]
Plaster	0.010	0.80	1.709
Solid brick	0.160	0.60	
Plaster	0.010	0.80	

Table 3. Partition design parameters of the ceilings.

Layers	Thickness [m]	Thermal Conductivity [W·m^{-1}·K^{-1}]	*U*-Value [W·m^{-2}·K^{-1}]
Reinforced concrete	0.300	1.60	2.581

Table 4. Partition design parameters of the ceilings to unheated attic.

Layers	Thickness [m]	Thermal Conductivity [W·m^{-1}·K^{-1}]	*U*-Value [W·m^{-2}·K^{-1}]
Polystyrene	0.100	0.04	0.346
Reinforced concrete	0.300	1.60	

Table 5. Partition design parameters of the ground slab.

Layers	Thickness [m]	Thermal Conductivity [W·m^{-1}·K^{-1}]	*U*-Value [W·m^{-2}·K^{-1}]
Concrete screed	0.080	1.60	0.230
Extruded polystyrene	0.120	0.03	
Bitumen	0.005	0.17	
Concrete	0.150	1.60	

2.3. Boundary Conditions

Selecting the right boundary conditions for calculating energy demand is a key issue. In the era of rapid climate change that is currently taking place, it is difficult to use so-called TMYs (Typical Meteorological Years). In order to minimize the possibility of making an incorrect selection of boundary conditions, three statistical climates were adopted for Kraków based on data from different periods [48]:

- TMY_1 based on data from 2004 to 2018;
- TMY_2 based on data from 2007 to 2021;
- TMY_3 based on data from 2009 to 2023.

These climates differ slightly from each other (Figure 6a). Based on the analysis of the main outdoor air parameters influencing heat exchange through the building envelope, it can be concluded that:

1. The average outside air temperature in Kraków has been systematically increasing over the last few years. The increase in this average is mainly caused by the increase in air temperatures in the summer. The difference in maximum temperature between TMY_3 and TMY_1 is 3 °C (Table 6). There was a more than three-fold increase in the share of temperatures above 30 (from 20 h for TMY_1 to 65 h for TMY_3).

2. Maximum solar radiation in all TMYs is at a similar level (Figure 6b). However, the number of hours with radiation has increased by about 5%.

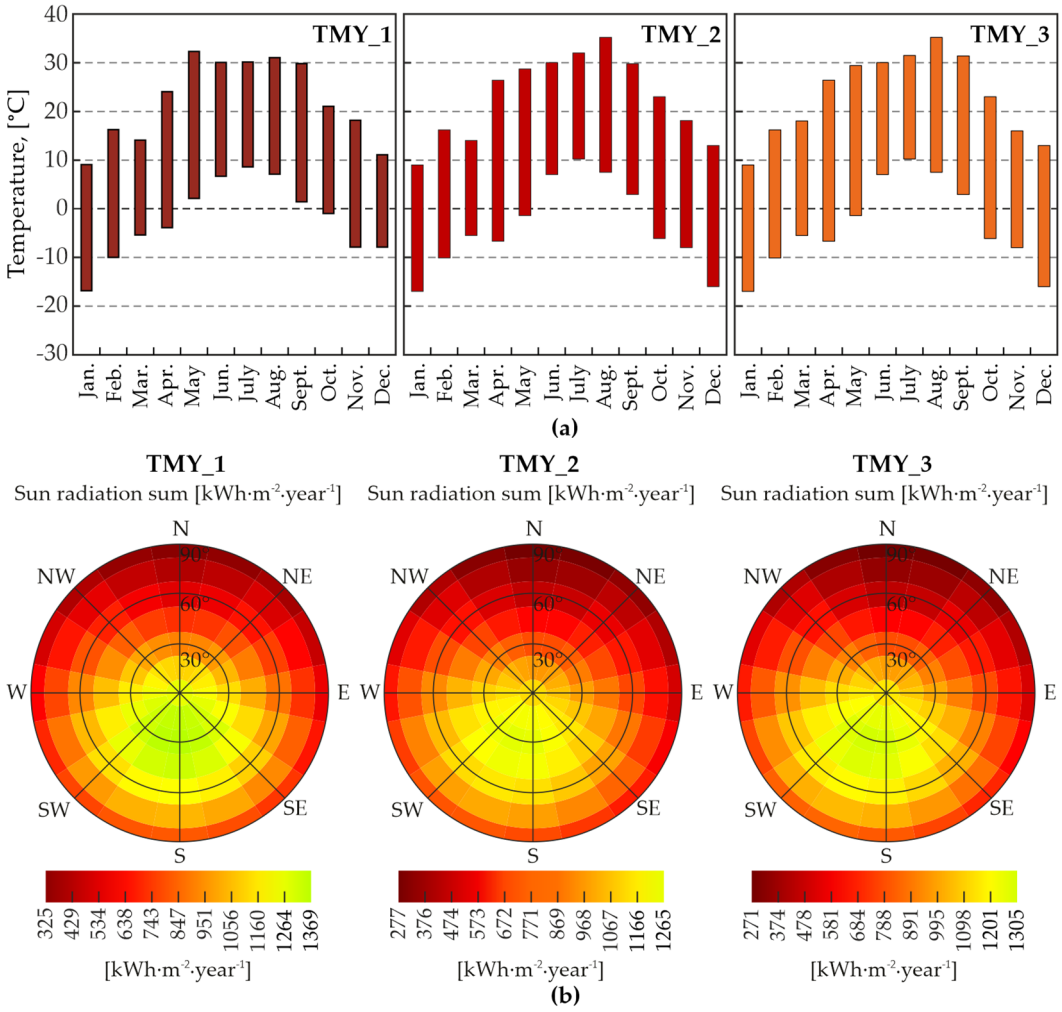

Figure 6. Outside air temperature extremes in individual months (**a**) as well as sun radiation sum depending on the angle of the surface and its orientation (**b**) for chosen TMYs.

Table 6. Basic statistics for temperature and solar radiation for TMYs.

Parameter	TMY_1	TMY_2	TMY_3
Maximum temperature [°C]	32.3	35.2	35.2
Minimum temperature [°C]	−17.0	−16.7	−17.0
Median for temperature [°C]	9.4	9.5	9.7
Maximum solar radiation [kW·m^{-2}·K^{-1}]	895	858	869
Hours of sun	4402	4614	4609

2.4. Internal Heat Gains

Internal heat gains were included in the calculations. Daily profiles from the database were adopted (for a 4-person family—see Figure 7). The maximum heat gains for individual simulated zones reach 9390 W on weekdays and 9735 W on weekends.

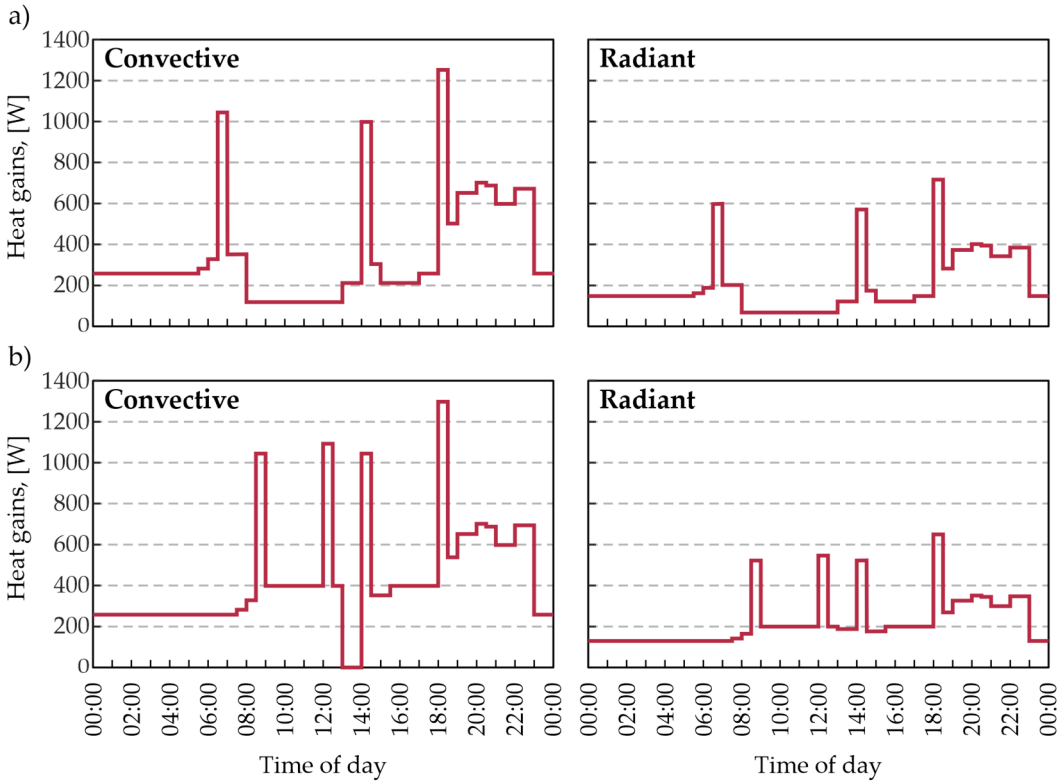

Figure 7. Heat gains of a single apartment for weekdays (**a**) and weekends (**b**).

2.5. HVAC and Ventilation Systems

To determine the energy demand for heating and cooling, the calculations assumed the operation of ideal (with infinite power) heating and cooling systems. For the thermal comfort of the users, the minimum permissible temperature was set at 20 °C and the maximum at 26 °C. The selected temperature range corresponds to the 2nd comfort class according to the standard EN 16798-1:2019 [49] (for residential buildings—sedentary activity about 1.2 met).

In terms of ventilation, it was assumed that the air exchange rate (*ACH*) resulting from infiltration was 0.1 and from gravity ventilation was 0.5.

2.6. Calculation Variants

In order to obtain complete data, calculations were performed for 6 variants for each of the statistical years (Table 7). In the methodology of calculating the heating load for design purposes, internal heat sources are not taken into account. Therefore, in the basic variants, only the empty building envelope is taken into account. Thus, ultimately 18 versions of calculations were performed.

Table 7. Variants of calculation.

Variant	Internal Heat Gains	HVAC Systems		Shading from Nearby Buildings
		Heating	Cooling	
V_1A	NO	NO	NO	NO
V_2A	NO	YES	NO	NO
V_3A	YES	YES	YES	NO
V_1B	NO	NO	NO	YES
V_2B	NO	YES	NO	YES
V_3B	YES	YES	YES	YES

3. Results

For the purpose of the data analysis, the building was divided into individual calculation zones corresponding to individual floors of the building (from Z_1 corresponding to the 1st floor to Z_5 corresponding to the 5th floor).

3.1. Internal Temperature

As a result of the calculations, the internal air temperature annual variations were obtained. Considering the only empty building envelope, in winter, regardless of TMY, the temperature inside the building drops below 0 °C. In summer, however, it does not exceed 25 °C. Figure 8 shows the example of the calculation results for TMY_3 (for Z_1 and Z_5, i.e., two extreme curves).

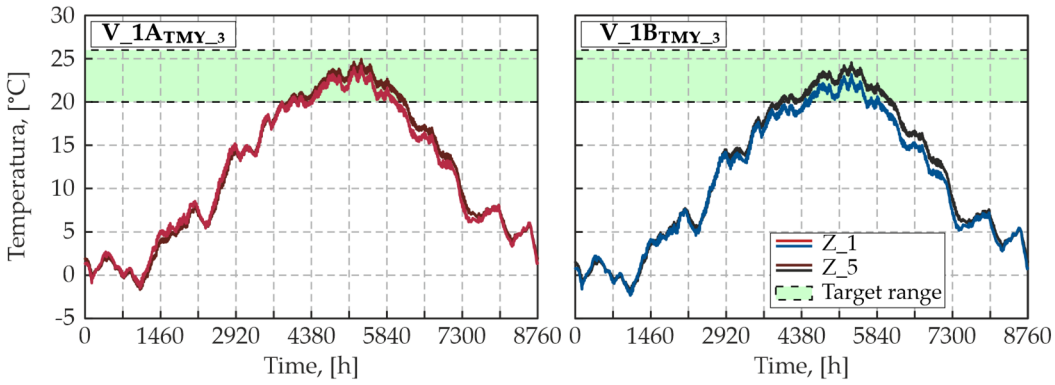

Figure 8. Internal air temperature of the first and fifth zones based on calculations that do not take into account (**left**) and take into account (**right**) shading from nearby buildings (TMY_3).

Depending on the building floor, for V_1A, the minimum temperatures for TMY_1 ranged from −2.1 °C to −1.9 °C, for TMY_2 from −2.5 °C to −2.4 °C, and for TMY_3 from −1.8 °C to −1.5 °C (Figure 9). After taking into account the shading from the nearby buildings (V_1B), these temperatures decreased even further: for TMY_1 it ranged from −2.7 °C to −2.4 °C, for TMY_2 from −3.4 °C to −2.9 °C, and for TMY_3 from −2.4 °C to −2.1 °C. For V_1A, the maximum temperatures for TMY_1 ranged from 23.9 °C to 24.7 °C, for TMY_2 and TMY_3 from 24.2 °C to 25.0 °C. For V_1B, similarly to V_1A, after taking into account shading, the temperatures decreased: for TMY_1 it ranged from 23.0 °C to 24.4 °C, and for TMY_2 and TMY_3 from 23.2 °C to 24.6 °C.

As can be seen from Figure 8 as well as Figure 9, the results obtained for the individual zones differ slightly from each other. However, they are highly correlated. The correlation coefficient between individual zones, for all the considered variants, is 0.999.

In the case of the analysed type of building in the climate conditions of Kraków, cooling is typically not used in the summer. In the case of passive microclimate shaping (without taking into account any internal heat gains), the temperature in this period is within the target range (Figure 8). However, after taking into account internal heat gains (for an additional calculation variant), as a result of the simulation, regardless of the selected TMY, the temperatures on all floors of the building exceeded the assumed upper limit of this range, i.e., 26 °C.

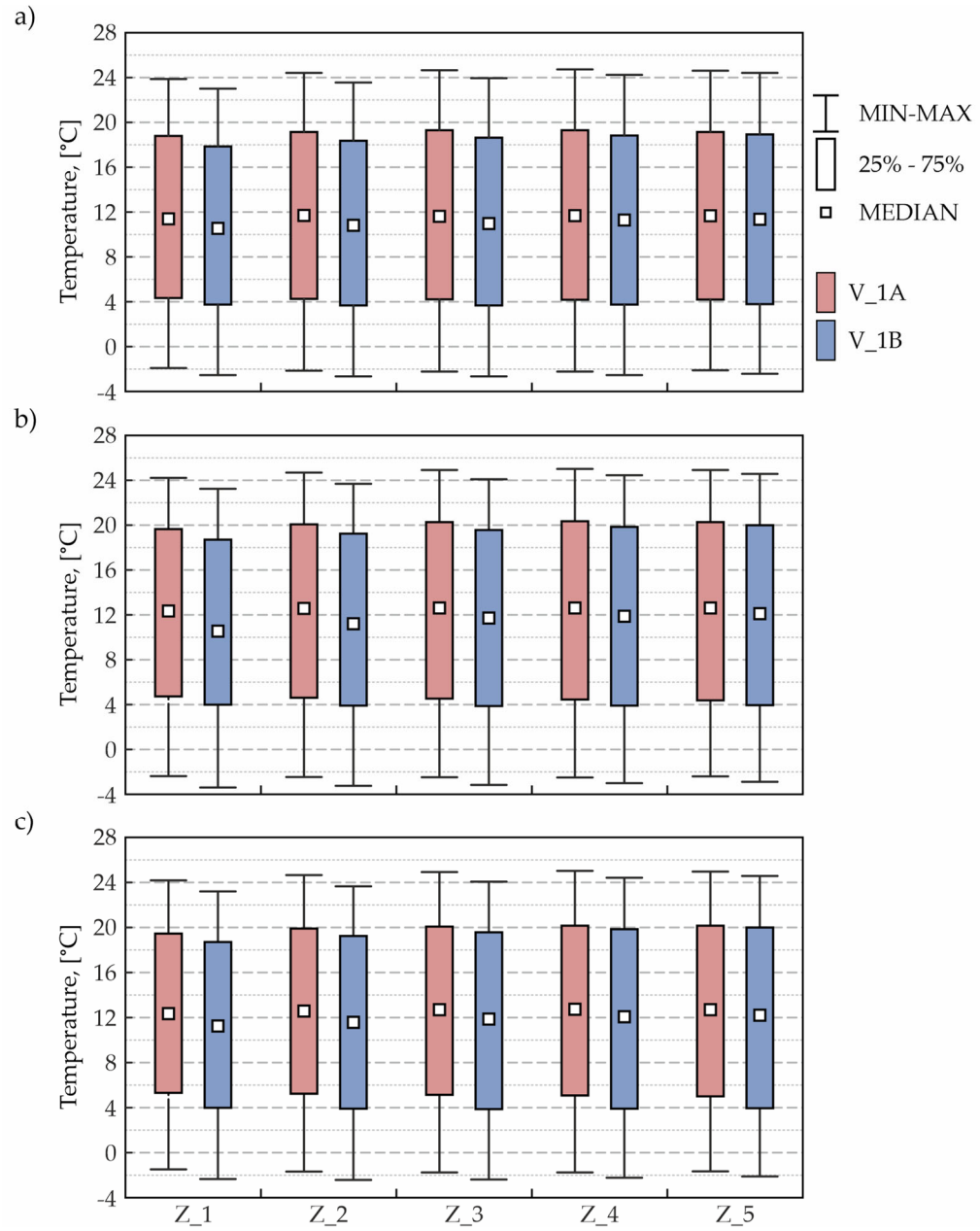

Figure 9. Basic descriptive statistics (location parameters) for internal air temperature (V_1A and V_1B) for chosen TMYs.

For variants where both heating and cooling systems are assumed, room temperature is maintained within the specified range. Due to the assumption of ideal systems, it is exactly 20 °C during the heating period and exactly 26 °C during the cooling period (Figure 10). After taking into account shading, the differences in indoor air temperature between individual zones are more visible (this applies to transitional periods when HVAC installations are not operating)—the temperatures on the lower floors are lower, with the average difference between Z_5 and Z_1 being 0.15 °C higher when taking into account shading (the maximum difference is 0.4 °C higher).

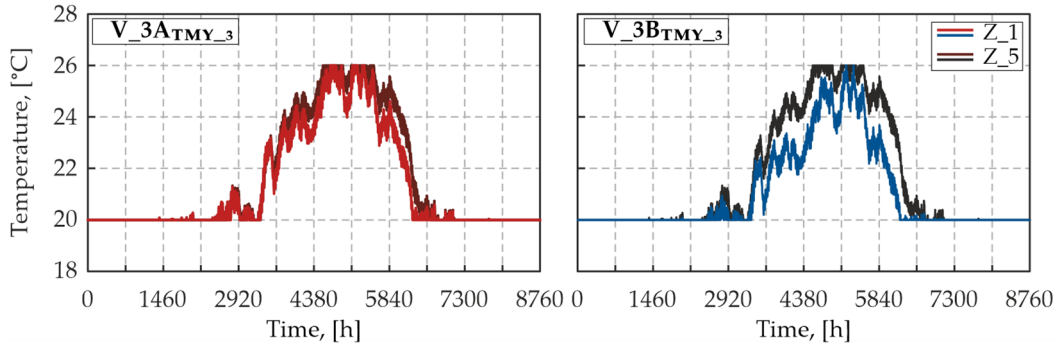

Figure 10. Internal temperature for Z_1 and Z_5 based on the calculations that take into account HVAC systems (heating and cooling), V_3A and V_3B for TMY_3.

3.2. Solar Heat Gains

As a result of the simulations, the solar heat gains were also determined. In the case of calculations without shading, for each floor (calculation zone) the maximum hourly solar heat gains were 13 kW for TMY_1 and 14 kW for TMY_2 as well as TMY_3. As can be seen in Figure 11, the variability patterns for individual zones are almost identical (within individual TMYs)—with a standard deviation of 3.65 kW. In the case of variants in which shading was taken into account, the solar heat gains differ depending on the zone. For this case, the maximum hourly heat gains and standard deviation are listed in Table 8.

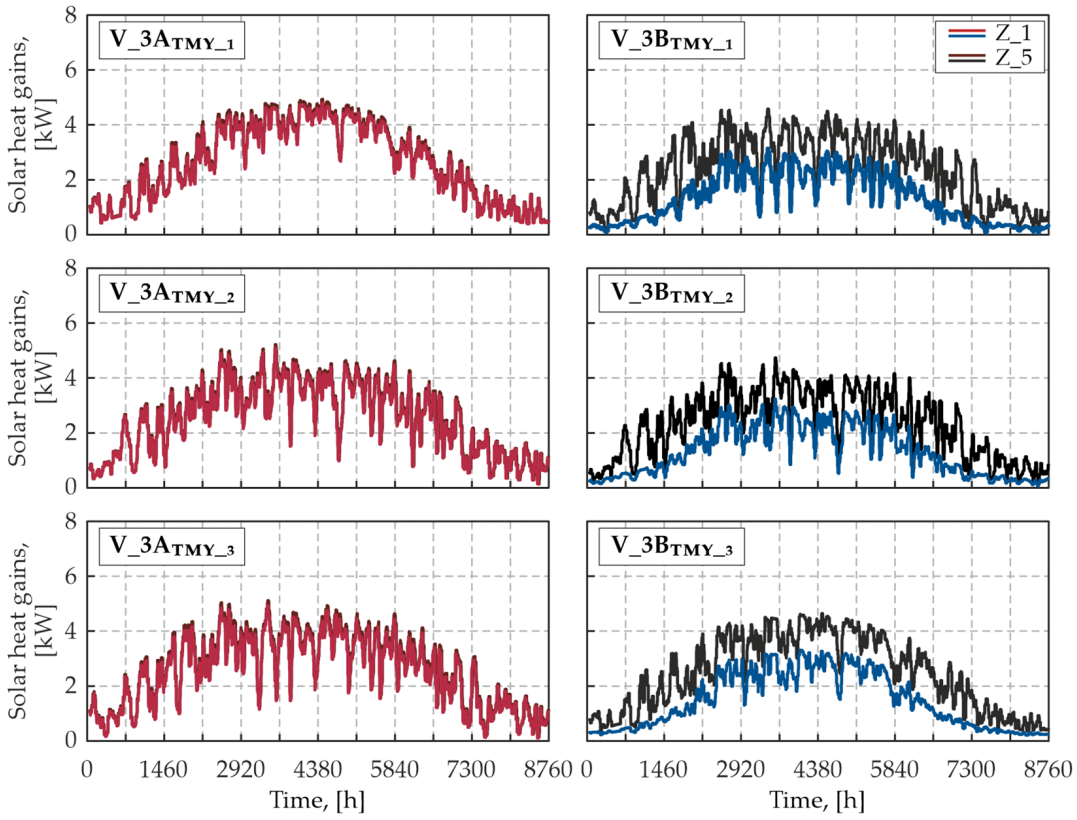

Figure 11. Moving average (48 h) of solar heat gains for Z_1 and Z_5 (the concept of moving average was used for the sake of clear graphical interpretation of the results), V_3A and V_3B for chosen TMYs.

Table 8. Maximum solar heat gains and standard deviation for V_3B.

External Climate	Maximum Solar Heat Gains, [kW]					Standard Deviation, [kW]				
	Z_1	**Z_2**	**Z_3**	**Z_4**	**Z_5**	**Z_1**	**Z_2**	**Z_3**	**Z_4**	**Z_5**
TMY_1	10.7	12.8	13.1	13.6	13.8	2.1	2.5	2.7	3.2	3.4
TMY_2	10.7	12.8	13.1	13.6	13.8	2.0	2.4	2.6	3.1	3.3
TMY_3	10.7	11.4	11.6	11.9	12.2	2.3	2.7	2.9	3.3	3.5

The medians of hourly solar heat gain values obtained for variant A were 5.1 kW for TMY_1, and 4.8 kW for TMY_2 and TMY_3. In the case of variant B, they differed depending on the zone:

- for TMY_1: 2.2 kW (for Z_1), 2.5 kW (Z_2), 2.8 kW (Z_3), 4.0 kW (Z_3) and 4.4 kW (Z_5);
- for TMY_2 and TMY_3: 1.9 kW (for Z_1), 2.1 kW (Z_2), 2.5 kW (Z_3), 3.6 kW (Z_3) and 4.1 kW (Z_5).

In case of the total (annual) value of the solar heat gains for the variants without considering shading, they amounted to 114,499 kW for TMY_1, 109,973 kW for TMY_2 and 112,496 kW for TMY_3. After considering the shading, they dropped to a level of 85,556 kW for TMY_1, 78,292 kW for TMY_2 and finally 80,107 for TMY_3.

The solar heat gains were also characterized by different levels and frequency of changes in individual zones. For the variants in which shading was not taken into account, the coefficient of variation is at the same level, i.e., 1.4. For the variants in which shading was taken into account, it is 1.57–1.60 for Z_1, 1.57–1.58 for Z_2, 1.54–1.55 for Z_3, 1.56–1.47 for Z_4 and 1.42–1.44 for Z_5 (Figure 12). This means that the lower the floor, the greater the variability in the solar heat gains.

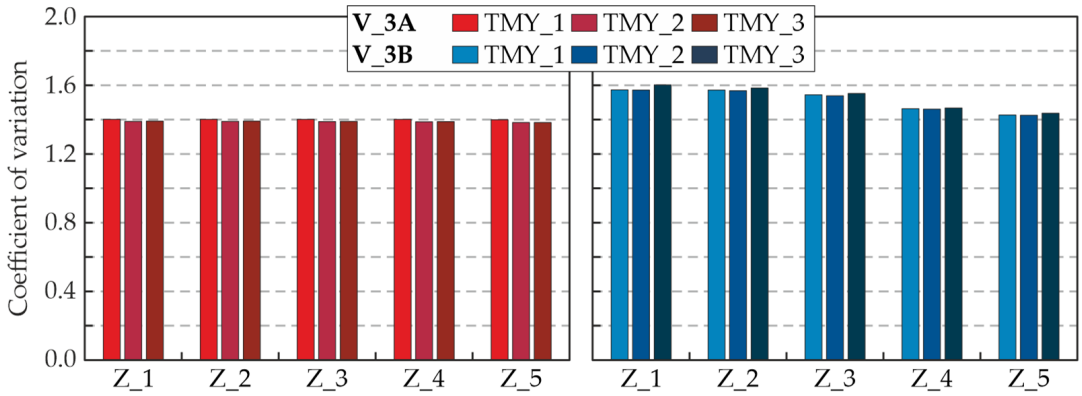

Figure 12. Coefficient of variation of solar heat gains for V_3A and V_3B for chosen TMYs.

3.3. Energy Demand

The energy demand for heating was determined based on variants V_2A and V_2B, while the energy demand for cooling was determined based on variants V_3A and V_3B. Heating and cooling power (per hour) during the calendar year for TMY_3 is illustrated in Figure 13.

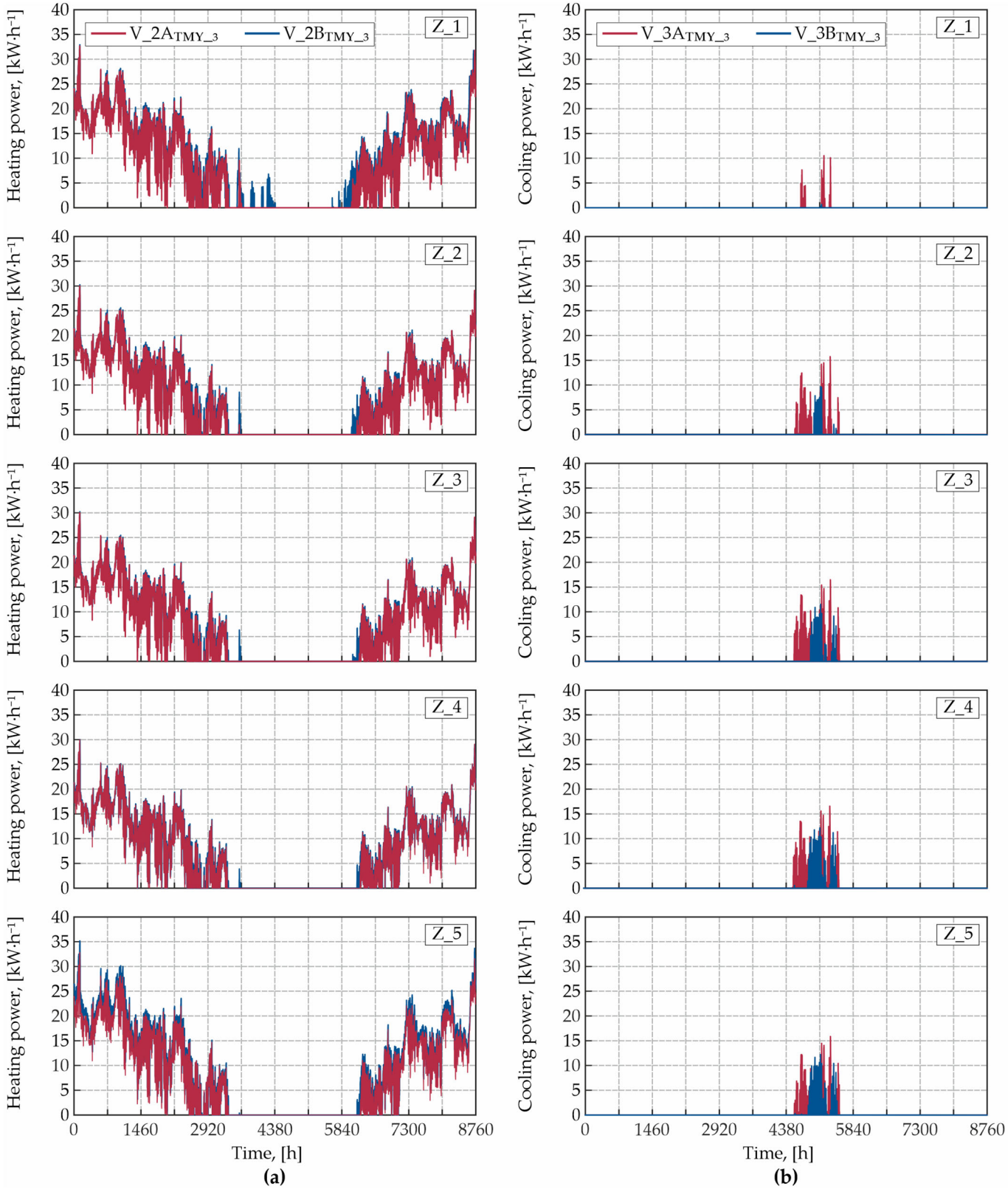

Figure 13. Heating power (V_2A and V_2B) (**a**) and cooling power (V_3A and V_3B) (**b**) for TMY_3.

3.3.1. Heating

In the case of the calculations without shading, no differences were noted between the maximum heating power for zones Z_2, Z_3 and Z_4. It was 30.3 kW·h^{-1} for TMY_1, 31.0 kW·h^{-1} for TMY_2 and 30.0 kW·h^{-1} for TMY_3 (Table 9). In the case of the 1st floor

(Z_1), the increase in heating power by an average of 2.63 kW·h^{-1} (average calculated from all TMYs) was influenced by the heat exchange through the floor to the ground. For Z_5, the increase of an average of 2.9 kW·h^{-1} was influenced by the heat exchange through the ceiling to the unheated attic. In the case of the calculations with shading, relatively small changes (of approx. 0.2 kW·h^{-1}) were observed between zones Z_2 and Z_4. Similarly, an increase in heating power was observed for the extreme zones. It amounted to an average of 2.63 kW·h^{-1} and 5.19 kW·h^{-1} for the first and top floors, respectively. It should be emphasized that the differences between individual TMYs are greater compared to the variants that do not take into account shading.

Table 9. Maximum heating power.

External Climate	Without Shading, [kW·h^{-1}]					With Shading, [kW·h^{-1}]				
	Z_1	**Z_2**	**Z_3**	**Z_4**	**Z_5**	**Z_1**	**Z_2**	**Z_3**	**Z_4**	**Z_5**
TMY_1	32.9	30.3	30.3	30.3	33.1	32.9	30.3	30.2	30.1	34.9
TMY_2	33.6	31.0	31.0	31.0	34.1	34.1	31.5	31.4	31.1	36.7
TMY_3	32.7	30.0	30.0	30.0	32.8	32.9	30.2	30.2	30.0	35.2

Obviously, the heating system does not operate at maximum power all the time. The values of the median of heating power for zones Z_2 to Z_4 are similar, regardless of TMY and whether shading has been taken into account or not. They remain within the range 12.4 to 12.8 kW·h^{-1} (Figure 14a). In the case of Z_1, the median is in the range of 14.4 to 14.7 kW·h^{-1} (except for variant V_2B for TMY_1 where it is 13.9 kW·h^{-1}). For zone Z_5, there is a clear difference between the variant V_2A (depending on TMY 14.5–14.6 kW·h^{-1}) and the one in which shading was taken into account depending on TMY 15.6–15.7 kW·h^{-1}).

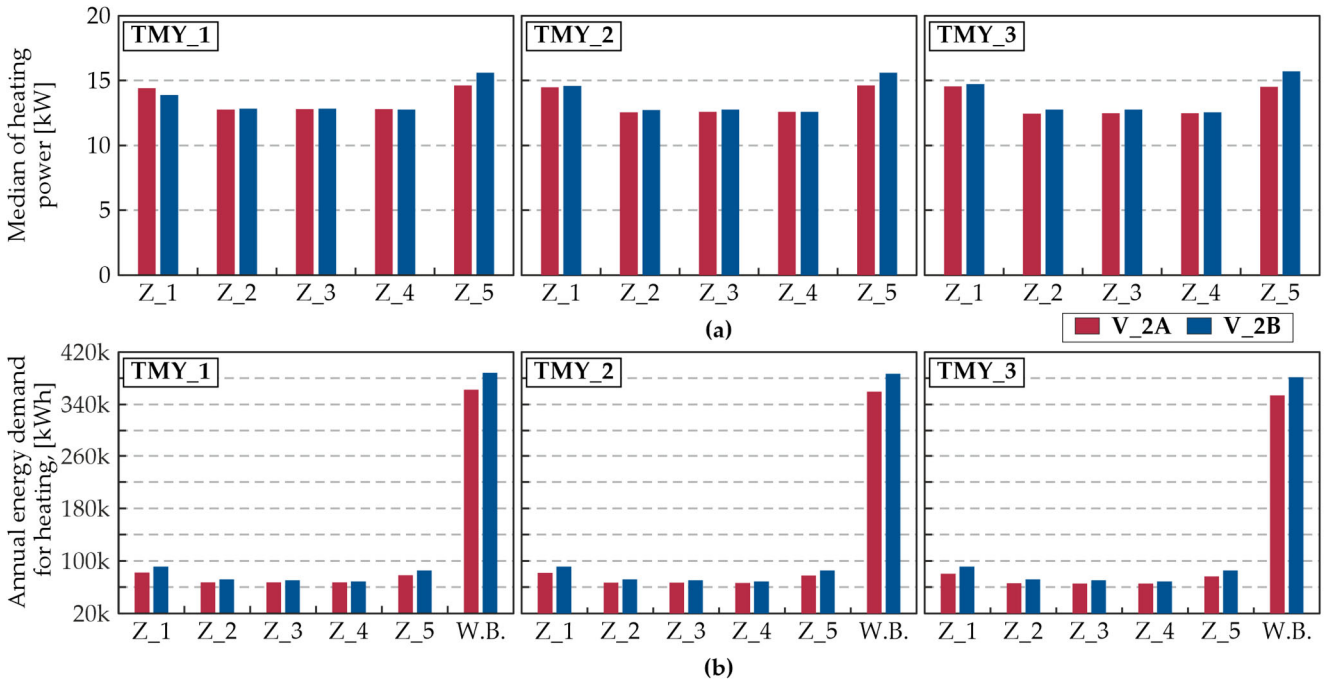

Figure 14. Median of heating power (**a**) and annual energy demand for heating (**b**), (V_2A and V_2B) for chosen TMYs for zones (Z_1–Z_5) and whole building (W.B.).

Taking into account the annual energy demand for heating, the differences between variants V_2A and V_2B are visible. Depending on TMY, for V_2A they remain in the following ranges (Figure 14b):

- 80,418–82,384 kWh for Z_1;
- 65,576–67,474 kWh for Z_2–Z_4;
- 76,384–78,138 kWh for Z_5.

These give the annual heating energy demand for the entire building (W.B in Figure 14b) at the level of 353,933–362,456 kW. For V_2B, where the differences between zones Z_2–Z_4 are visible, the results were as follows:

- 88,610–91,427 kWh for Z_1;
- 71,451–72,388 kWh for Z_2;
- 69,957–70,962 kWh for Z_3;
- 67,575–68,664 kWh for Z_4;
- 84,066–85,456 kWh for Z_5.

These figures give the annual heating energy demand for the entire building at the level of 381,659–388,248 kWh. The lowest demand was recorded for TMY_3 and the highest for TMY_1.

3.3.2. Cooling

In the case of cooling power, regardless of whether the shading from nearby buildings is taken into account or not, there are differences depending on the floors. They are the result of increased heat exchange between the outer floors and the surroundings (ground and unheated attic), which influences the heat exchange between the middle floors. The maximum cooling power is presented in Table 10. In the absence of shading, it assumes values in the range 7.0–12.8 kW·h^{-1} for TMY_1, 10.8–17.0 kW·h^{-1} for TMY_2 and 10.5–16.6 kW·h^{-1} for TMY_3. After taking into account shading, the cooling power decreased significantly for the lower floors and only slightly for the top floor. The ranges in this case are 0.7–12.3 kW·h^{-1} for TMY_1, 4.7–15.7.0 kW·h^{-1} for TMY_2 and 2.8–15.7 kW·h^{-1} for TMY_3.

Table 10. Maximum cooling power.

External Climate	Without Shading, [kW·h^{-1}]					With Shading, [kW·h^{-1}]				
	Z_1	**Z_2**	**Z_3**	**Z_4**	**Z_5**	**Z_1**	**Z_2**	**Z_3**	**Z_4**	**Z_5**
TMY_1	7.0	12.3	12.8	12.8	12.3	0.7	9.7	11.5	12.2	12.3
TMY_2	10.8	15.8	17.0	16.6	15.8	4.7	12.1	14.8	15.7	15.4
TMY_3	10.5	15.7	16.5	16.6	15.9	2.8	12.0	14.8	15.7	15.3

In the case of the calculations for cooling, the differences related to the TMY, used as the boundary conditions, are clearly visible. However, in each case there is a clearly visible reduction in cooling power for the variants taking into account shading (Figure 15a). The greatest differences between variants A and B were noted for the lower floors:

1. for TMY_1:
   - for variant without shading (variant V_3A): 1.9 kW·h^{-1} for Z_1, 7.2 kW·h^{-1} for Z_2, and 7.6 kW·h^{-1} for Z_3 as well as Z_4, and 7.1 kW·h^{-1} for Z_5;
   - for variant with shading (variant V_3B): 0.7 kW·h^{-1} for Z_1, 3.7 kW·h^{-1} for Z_2, 5.8 kW·h^{-1} for Z_3, 7.0 kW·h^{-1} for Z_4 and 6.8 kW·h^{-1} for Z_5,
2. for TMY_2:
   - for variant V_3A: 3.2 kW·h^{-1} for Z_1, 4.7 kW·h^{-1} for Z_2, 4.3 kW·h^{-1} for Z_3, 4.2 kW·h^{-1} for Z_4 and 4.5 kW·h^{-1} for Z_5;
   - for variant V_3B: 2.1 kW·h^{-1} for Z_1, 3.5 kW·h^{-1} for Z_2, 3.8 kW·h^{-1} for Z_3, 4.2 kW·h^{-1} for Z_4 and 4.4 kW·h^{-1} for Z_5,
3. for TMY_3:
   - for variant V_3A: 2.6 kW·h^{-1} for Z_1, 3.6 kW·h^{-1} for Z_2, 4.1 kW·h^{-1} for Z_3, 4.2 kW·h^{-1} for Z_4 and 3.9 kW·h^{-1} for Z_5;

- for variant V_3B: 0.7 kW·h^{-1} for Z_1, 2.6 kW·h^{-1} for Z_2, 3.4 kW·h^{-1} for Z_3, 3.6 kW·h^{-1} for Z_4 and 3.4 kW·h^{-1} for Z_5.

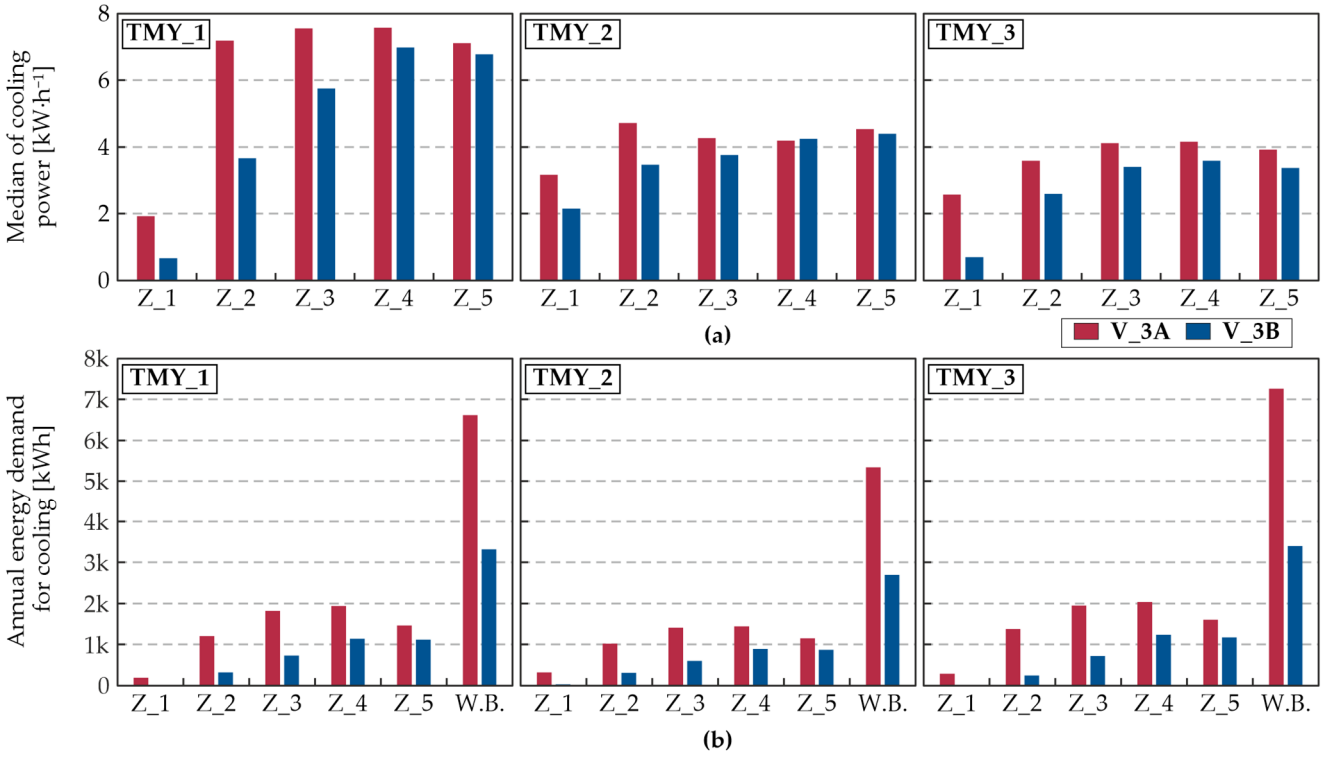

Figure 15. Median of cooling power (**a**) and annual energy demand for cooling (**b**), (V_3A and V_3B) for chosen TMYs for zones (Z_1–Z_5) and whole building (W.B.).

Taking into account the annual energy demand for cooling, the differences between variants V_3A and V_3B are clearly visible. Depending on the TMY, for V_3A they amount to the following (Figure 15b):

- 193–322 kWh for Z_1;
- 1023–1382 kWh for Z_2;
- 1408–1952 kWh for Z_3;
- 1442–2042 kWh for Z_4;
- 1151–1601 kWh for Z_5.

These figures give the annual cooling energy demand for the entire building (W.B at Figure 15b) at the level of 5347–7269 kWh. For V_3B, where the differences between zones Z_2–Z_4 are visible, the following figures were obtained:

- 1–25 kWh for Z_1;
- 248–323 kWh for Z_2;
- 603–737 kWh for Z_3;
- 892–1237 kWh for Z_4;
- 783–1178 kWh for Z_5.

These figures give the annual cooling energy demand for the entire building at the level of 2702–3398 kWh. The lowest demand was recorded for TMY_2 and the highest for TMY_3.

4. Discussion of the Results

The analysed building is located in a temperate climate, where heating is a key issue. However, calculations have confirmed that in the era of climate warming, in order to maintain thermal comfort conditions, cooling is also necessary. Based on the projected climate changes in Central Europe, regardless of the climate change scenario, increasingly

longer heat waves with increasingly higher temperatures are predicted. As a consequence, higher temperatures are expected to cause a shift in the geographical distribution of climate zones [50]. According to data collected in various parts of the world, climate change has caused an increase in the frequency, duration and intensity of heat waves [51,52]. Therefore, a multi-criteria approach to managing and optimizing energy consumption in buildings is important. As the analysis of the results shows, taking into account the shading from nearby buildings may be crucial for optimizing the volume (power of devices, diameters of ducts and pipes) of the HVAC installation.

In the analysed case, the value of the inverted aspect ratio H/W for the modelled building with its surroundings is 1.11 for both the north–south and east–west axes. This value, as given by [53], is similar to the value for regular urban canyons, where the H/W values are 0.5 for avenue-type canyons, 1.0 for regular canyons with a similar building height and street width, and values above 2.0 for deep canyons. In [54], it was pointed out that H/W is more important than orientation. For this reason, changes in building orientation were not tested.

In the discussed case, the annual energy demand for heating, after considering the shading, increased by 7% for TMY_1 (25,793 kWh) and by 8% (27,505 kWh) for TMY_2 and TMY_3 (27,726 kWh). Considering the division of the building into zones, the calculations show that the increase in energy demand for heating also depends on the floor. It is as follows:

- for TMY_1: 11% for Z_1, 7% for Z_2, 5% for Z_3, 2% for Z_4 and 9% for Z_5;
- for TMY_2: 10% for Z_1, 8% for Z_2, 6% for Z_3, 3% for Z_4 and 10% for Z_5;
- for TMY_3: 10% for Z_1, 8% for Z_2, 7% for Z_3, 3% for Z_4 and 10% for Z_5.

For all TMYs, the results for individual zones are similar. The greatest increase in demand for heating is observed on the outer floors, while the smallest is observed on the middle floor, i.e., where the climate is stabilized by the adjacent heated zones.

In the case of energy demand for cooling, as was to be expected, a decrease was noted after considering shading: 50% for TMY_1 (3302 kWh), 49% for TMY_2 (2645 kWh) and finally 53% for TMY_3 (3871 kWh). Similarly to the heating, in this case there were differences for the zones as follows:

- for TMY_1: 99% for Z_1, 73% for Z_2, 59% for Z_3, 41% for Z_4 and 24% for Z_5;
- for TMY_2: 92% for Z_1, 70% for Z_2, 57% for Z_3, 38% for Z_4 and 24% for Z_5;
- for TMY_3: 95% for Z_1, 82% for Z_2, 63% for Z_3, 39% for Z_4 and 26% for Z_5.

For all TMYs, the results for individual zones are similar. The greatest decrease in demand for cooling is observed on the bottom floors, while the smallest is observed on the top floor.

The 8% increase in energy demand for heating and 50% decrease in energy demand for cooling obtained from the calculations are confirmed in the literature. These results cannot be extrapolated directly to those obtained for hot or cold climates, which are the focus of most publications (e.g., shading studies showed that energy demand decreases by 42% in summer in Miami and increases by 22% in winter in Minneapolis [31]), but according to [27], for a building analysed in a moderate climate with H/W equal to 2.0, the increase in the energy demand for heating, after considering shading, reaches 26.3% and the decrease in the energy demand for cooling reaches 53.6%. Therefore, the depth of the urban canyon will have a significant impact on the differences in the building's demand for energy needed for heating and cooling. This relationship in Poland was also confirmed in [55] (pp. 107–116).

As shown by the detailed analysis of the maximum energy demand, considering shading has less impact on the size of the designed installation in the case of heating than cooling (because these systems are designed for maximum heat losses and gains). For heating, the average increase in the maximum energy demand for all the tested outdoor climates was 0.6% for all zones except the top floor (Z_5), for which the increase was 6.8%.

For cooling, greater variability was observed. Related to both the change in zone and external climate, maximum energy demand decreased by the following:

- for TMY_1: 87% for Z_1, 21% for Z_2, 10% for Z_3, 5% for Z_4 and for Z_5 remained unchanged;
- for TMY_2: 57% for Z_1, 23% for Z_2, 13% for Z_3, 5% for Z_4 and 3% for Z_5;
- for TMY_3: 73% for Z_1, 24% for Z_2, 10% for Z_3, 5% for Z_4 and 3% for Z_5.

The differences in the results for individual calculation zones confirm the necessity of such divisions, even for relatively low buildings. As shown in the results of previous research [30], division into individual storeys is sufficient. It should be emphasized that in the case of calculations used in the dimensioning of air-conditioning installations, the division of individual storeys into smaller calculation zones should be considered (due to the high dependence of heat gains on solar radiation).

It should be noted that the annual energy demand for both processes is influenced by the operating time of the devices, in addition to the hourly energy demand. As can be seen in the example of TMY_3 (Figure 16), considering shading resulted in an increase in the operating time of heating devices and a reduction in the operating time of cooling devices. In case of heating the percentage of equipment operating time during the year increased as follows:

- for TMY_1: from 59.1% to 62.8% for Z_1, from 54.0% to 57.2% for Z_2, from 53.5% to 57.2% for Z_3, from 53.4% to 54.4% for Z_4 and from 55.6% to 56.2% for Z_5;
- for TMY_1: from 57.5% to 62.8% for Z_1, from 52.8% to 56.9% for Z_2, from 50.0% to 55.5% for Z_3, from 52.1% to 54.2% for Z_4 and from 53.7% to 56.2% for Z_5;
- for TMY_1: from 58.1% to 63.7% for Z_1, from 52.7% to 57.8% for Z_2, from 51.9% to 56.7% for Z_3, from 52.9% to 55.4% for Z_4 and from 53.7% to 57.9% for Z_5.
- In the case of cooling, the changes in percentage are as follows:
- for TMY_1: from 0.9% to 0.1% for Z_1, from 3.3% to 0.8% for Z_2, from 4.9% to 2.1% for Z_3, from 5.2% to 3.3% for Z_4 and from 4.2% to 3.2% for Z_5;
- for TMY_1: from 0.9% to 0.1% for Z_1, from 2.2% to 0.8% for Z_2, from 3.2% to 1.5% for Z_3, from 3.3% to 2.1% for Z_4 and from 2.5% to 2.1% for Z_5;
- for TMY_1: from 1.0% to 0% for Z_1, from 3.6% to 1.1% for Z_2, from 4.7% to 2.3% for Z_3, from 4.8% to 3.1% for Z_4 and from 4.0% to 3.1% for Z_5.

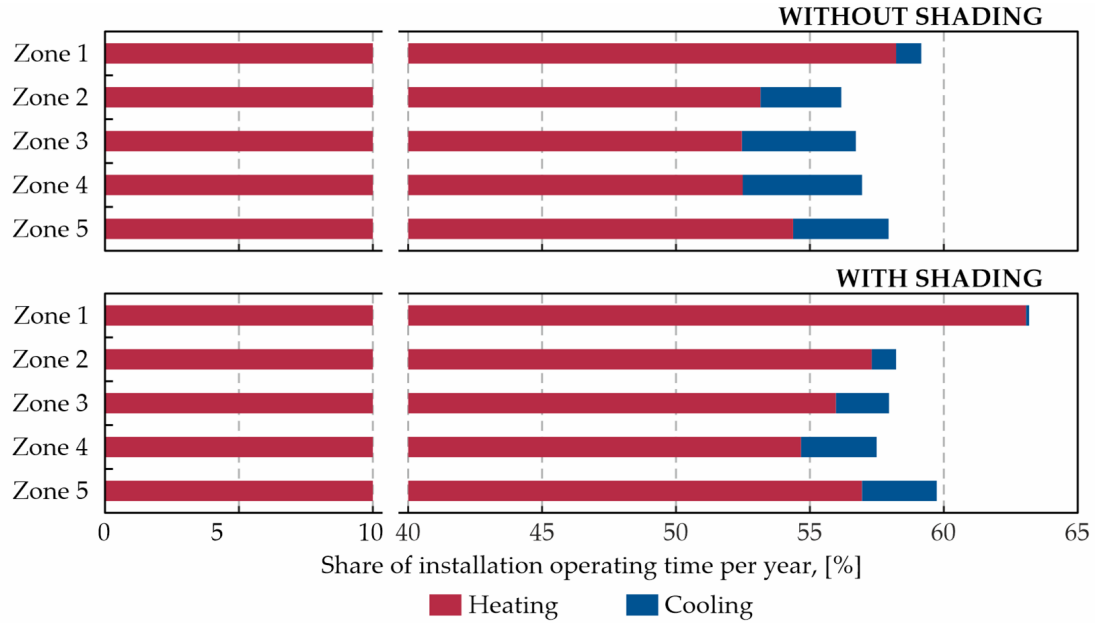

Figure 16. Percentage of heating and cooling devices operating time per year for TMY_3.

The maximum hourly energy demand values can be compared to the heating and cooling power. Design heat load is defined as the heat flow (power) required to achieve the specified internal design temperature under external design conditions. For the whole building, it is calculated from all transmission heat losses to the exterior and the ventilation heat loss of the building and with or without additional heating power. As a result of the calculations carried out (according to [11,12]), without taking into account the heating power, for the middle floor (Z_3) of the analysed building, a value of 38.3 kW was obtained. This means that in the case of steady-state calculations, 22–28% higher heating load (depending on TMY) values were obtained. It should be emphasized, however, that the calculations were performed at the currently applicable calculation temperature for winter, which is −20 °C for Kraków. In the case of calculations made assuming a designed outside temperature of −17 °C (minimum temperature for the assumed statistical climates) the heating load decreased to 35.4 kW. In this case, the heating load obtained was higher than for transient calculations by 13–18%.

There are many methods for sizing HVAC systems. A review of the calculation methods used for this purpose can be found in [56,57]. In Poland, the calculation methodology proposed in [58–60] is commonly used. Based on calculations made according to this method, assuming internal heat gains at the level of 9.8 kW (which corresponds to the maximum heat gains assumed in transient calculations), the cooling load for Z_3 is 51 kW. Therefore, it can be stated that the transient calculations gave a result that was 64–73% lower for the variant without shading and 71–77% with shading. Such large differences result from the fact that constant (lasting throughout the day) internal heat gains were assumed in the calculations and also from the estimated determination of the building's thermal storage capacity.

Due to the fact that the analysed building is generic, it was impossible to validate and calibrate the model. The calculations also assume that HVAC systems operate without any losses. Therefore, the energy demand results cannot be considered final. The accuracy of the predictions is also influenced by the adoption of a simplified scheme of internal heat and moisture gains. As the analyses show, their impact on the demand for energy for cooling is significant. In variants where internal heat gains were not taken into account (e.g., V_1A and V_1B), the calculated internal temperature in the summer period did not exceed the permissible range (Figure 8). Therefore, according to these variants, for the assumed external climates, there was no need for cooling. Nevertheless, adopting the above-described simplifications allows for the formulation of generalized conclusions.

It should also be emphasized that the use of statistical climates affects the calculated energy demand (for heating and cooling) and loads. Observations of the actual climate in Kraków show that in recent years it has been significantly warmer than statistical climates, with long heat waves (in studies concerning Poland, a heat wave is often defined as a series of at least 3 days with maximum air temperature above 30 °C on each day) and tropical nights (by definition, a tropical night is when the air temperature does not drop below 20 °C throughout the night). For example, according to TMY_3, no tropical night is expected in July. In reality, a series of 6 nights in a row with temperatures not falling below 18 °C (in Polish conditions—a very warm night) was recorded in July 2024 (Figure 17). Three of them were tropical.

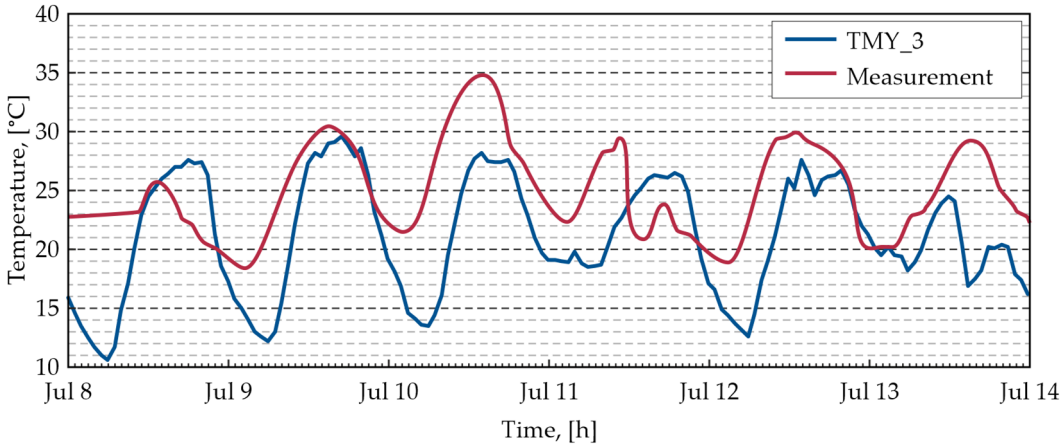

Figure 17. External air temperature according to TMY_3 against the temperature measured in Kraków on 8–13 July 2024.

5. Conclusions

The above analysis shows that considering shading from nearby buildings in the calculations of energy and power demand can significantly affect these calculations even in moderate climates. It also shows that the division of buildings into individual floors is equally important. The accuracy of the calculations not only impacts the system size but also influences the building's performance over the long run since oversized or undersized HVAC systems can exhibit less than optimal operation [56].

In temperate climates, the influence of shading in urban areas cannot be neglected in the calculation of energy demand for heating and cooling as well as in load calculation. In the case of a typical five-floor residential tenement house from the turn of the 20th century in Kraków, an 8% increase in energy demand for heating and a 50% reduction in energy demand for cooling were estimated.

The use of steady-state calculations (without considering shading from nearby buildings) may lead to oversizing the air conditioning systems on the lowest floors of the building. However, determining the exact oversizing requires further research.

In calculations, it is advisable to introduce separate calculation zones for each floor.

Author Contributions: Conceptualization: A.S.-S.; methodology: A.S.-S. and K.W.; formal analysis: A.S.-S. and K.W.; data curation: A.S.-S. and K.W.; writing—original draft preparation: A.S.-S.; writing—review and editing: A.S.-S. and K.W.; visualization: A.S.-S. and K.W. All authors have read and agreed to the published version of the manuscript.

Funding: This research received no external funding.

Data Availability Statement: The data presented in this study are available on request from the corresponding author.

Conflicts of Interest: The authors declare no conflicts of interest.

References

1. Kudas, D.; Wnęk, A.; Hudecová, Ľ.; Fencik, R. Spatial Diversity Changes in Land Use and Land Cover Mix in Central European Capitals and Their Commuting Zones from 2006 to 2018. *Sustainability* **2024**, *16*, 2224. [CrossRef]
2. Wnęk, A.; Kudas, D.; Stych, P. National Level Land-Use Changes in Functional Urban Areas in Poland, Slovakia and Czechia. *Land* **2021**, *10*, 39. [CrossRef]
3. Kudas, D.; Wnęk, A.; Tátošová, L. Land Use Mix in Functional Urban Areas of Selected Central European Countries from 2006 to 2012. *Int. J. Environ. Res. Public Health* **2022**, *19*, 15233. [CrossRef] [PubMed]
4. *EU/2024/1275*; Energy Performance of Buildings Directive. European Parliament and of the Council: London, UK, 2024.
5. Martínez-Molina, A.; Tort-Ausina, I.; Cho, S.; Vivancos, J.-L. Energy efficiency and thermal comfort in historic buildings: A review. *Renew. Sustain. Energy Rev.* **2016**, *61*, 70–85. [CrossRef]
6. Prömmel, A. Increased energy efficiency in existing buildings. *Habitat Int.* **1978**, *3*, 569–575. [CrossRef]

7. Johnsen, K. Energy conservation in the built environment. *Build. Environ.* **1980**, *15*, 15.
8. Tejani, A. Integrating Energy-Efficient HVAC Systems into Historical Buildings: Challenges and Solutions for Balancing Preservation and Modernization. *ESP JETA* **2021**, *1*, 83–97.
9. Szecskő, H.; Horváth, T. Challenges and opportunities in the energetic modernization of historic residential buildings in Budapest downtown. In Proceedings of the International Conference on New Energy and Future Energy Systems (NEFES 2024), Győr, Hungary, 29 July–1 August 2024.
10. *EN ISO 52016-1*; Energy Performance of Buildings. Calculation of the Energy Needs for Heating and Cooling, Internal Temperatures and Heating and Cooling Load in a Building or Building Zone—Part 1: Calculation Procedures. European Committee for Standardization: Brussels, Belgium, 2017.
11. *Environmental Design: CIBSE Guide A*; Chartered Institution of Building Services Engineers: London, UK, 2021.
12. *EN 12831:2003*; Heating Systems in Buildings—Method for Calculation of the Design Heat Load. European Committee for Standardization: Brussels, Belgium, 2003.
13. Vartholomaios, A. A parametric sensitivity analysis of the influence of urban form on domestic energy consumption for heating and cooling in a Mediterranean city. *Sustain. Cities Soc.* **2017**, *28*, 135–145. [CrossRef]
14. Liu, H.; Pan, Y.; Yang, Y.; Huang, Z. Evaluating the impact of shading from surrounding buildings on heating/ cooling energy demands of different community forms. *Build. Environ.* **2021**, *206*, 108322. [CrossRef]
15. Ichinose, T.; Lei, L.; Lin, Y. Impacts of shading effect from nearby buildings on heating and cooling energy consumption in hot summer and cold winter zone of China. *Energy Build.* **2017**, *136*, 199–210. [CrossRef]
16. Santamouris, M.; Asimakopoulos, D. *Energy and Climate in the Urban Built Environment*, 1st ed.; James & James: London, UK, 2001.
17. Johnson, G.; Watson, I. The determination of View-Factors in Urban Canyons. *J. Appl. Meteorol. Climatol.* **1984**, *23*, 329–335. [CrossRef]
18. Matzarakis, A.; Matuschek, O. Estimation of Sky View Factor in Urban Environments. Available online: https://www.researchgate.net/publication/267944926_Estimation_of_Sky_View_Factor_in_urban_environments (accessed on 11 November 2024).
19. Beckers, B. Geometrical Interpretation of Sky Light in Architecture Projects. Available online: http://www.heliodon.net/downloads/Beckers_2007_Helio_001_en.pdf (accessed on 11 November 2024).
20. Ali-Toudert, F.; Mayer, H. Effects of asymmetry, galleries, overhanging facedes and vegetation on thermal comfort in urban street canyons. *Sol. Energy* **2007**, *81*, 742–754. [CrossRef]
21. Johansson, E. Influence of the urban geometry on outdoor thermal comfort in a hot dry climate: A study in Fez, Morocco. *Build. Environ.* **2006**, *41*, 1326–1338. [CrossRef]
22. Huang, Y.; Akbari, H.; Taha, H.; Rosenfeld, A. The potential of vegetation in reducing summer cooling loads in residential buildings. *J. Appl. Meteorol.* **1987**, *26*, 1103–1116. [CrossRef]
23. Oke, T. Street design and urban canopy layer climate. *Energy Build.* **1988**, *11*, 103–113. [CrossRef]
24. Arnfield, J. Street design and urban canyon solar access. *Energy Build.* **1990**, *14*, 117–131. [CrossRef]
25. Lam, J. Shading effects due to nearby buildings and energy implications. *Energy Convers. Manag.* **2000**, *41*, 647–659. [CrossRef]
26. Danny, H.; Li, W.; Wong, S. Daylighting and energy implications due to shading effects from nearby buildings. *Appl. Energy* **2007**, *84*, 1199–1209.
27. Han, Y.; Taylor, J.; Pisello, A. Exploring mutual shading and mutual reflection inter-building effects on building energy performance. *Appl. Energy* **2017**, *185*, 1556–1564. [CrossRef]
28. Ali, U.; Shamsi, M.H.; Hoare, C.; Mangina, E.; O'Donnell, J. Review of urban building energy modeling (UBEM) approaches, methods and tools using qualitative and quantitative analysis. *Energy Build.* **2021**, *246*, 111073. [CrossRef]
29. Frayssinet, L.; Merlier, L.; Kuznik, F.; Hubert, J.L.; Milliez, M.; Roux, J.J. Modeling the heating and cooling energy demand of urban buildings at city. *Renew. Sustain. Energy Rev.* **2018**, *81*, 2318–2327. [CrossRef]
30. Faure, X.; Johansson, T.; Pasichnyi, O. The Impact of Detail, Shadowing and Thermal Zoning Levels on Urban Building Energy Modelling (UBEM) on a District Scale. *Energies* **2022**, *15*, 1525. [CrossRef]
31. Pisello, A.; Taylor, J.; Xu, X. Inter-building effect: Simulating the impact of a network of buildings on the accuracy of building energy performance predictions. *Build. Environ.* **2012**, *58*, 37–45. [CrossRef]
32. Bludau, C. Shading of flat roofs. In Proceedings of the 2nd International Conference on Moisture in Buildings (ICMB23), Online, 3–4 July 2023.
33. Wen, J.; Xie, Y.; Yang, S.; Yu, J.; Lin, B. Study of surrounding buildings' shading effect on solar radiation through. *Sustain. Cities Soc.* **2022**, *86*, 104143. [CrossRef]
34. Natanian, J.; Wortmann, T. Simplified evaluation metrics for generative energy-driven urban design. *Energy Build.* **2021**, *240*, 110916. [CrossRef]
35. Nawalany, G.; Sokołowski, P.; Lendelova, J.; Zitnak, M.; Jakubowski, T.; Atilgan, A. Numerical analysis of the heat exchange model with the ground on the example of a complex of industrial halls. *Energy Build.* **2023**, *300*, 113689. [CrossRef]
36. Wijesuriya, S.; Tabares-Velasco, P.C.; Biswas, K.; Heim, D. Empirical validation and comparison of PCM modeling algorithms commonly used in building energy and hygrothermal software. *Build. Environ.* **2020**, *73*, 106750. [CrossRef]
37. Staszczuk, A.; Kuczyński, T.; Wojciech, M.; Ziembicki, P. Comparative Calculation of Heat Exchange with the Ground in Residential Building Including Periodes of Heat Waves. *CEER* **2016**, *21*, 109–119. [CrossRef]

38. Coelho, G.; Silva, H.; Henriques, F. Development of a three-dimensional hygrothermal model of a historic building in WUFI®Plus vs EnergyPlus. In *MATEC Web of Conferences 282, Proceedings of the International Conference of 4th Central European Symposium on Building Physics (CESBP 2019), Prague, Czech Republic, 2–5 September 2019*; EDP Sciences: Les Ulis, France, 2019; p. 02079.
39. Lissner, J.; Kaiser, U.; Kilian, R. *Built Cultural Heritage in Times of Climate Change*; Fraunhofer-Center for Central and Eastern Europe MOEZ: Leipzig, Germany, 2014.
40. Sadłowska-Sałęga, A.; Radoń, J.; Sobczyk, J.; Wąs, K. Influence of microclimate control scenarios on energy consumption in the Gallery of the 19th-Century Polish Art in the Sukiennice (the former Cloth Hall) of The National Museum in Krakow. *IOP Conf. Ser. Mater. Sci. Eng.* **2018**, *415*, 012026. [CrossRef]
41. Radoń, J.; Sadłowska-Sałęga, P.; Wąs, K.; Gryc, A.; Kupczak, A. Energy use optimization in the building of National Library. *IOP Conf. Ser. Mater. Sci. Eng.* **2018**, *415*, 012029. [CrossRef]
42. Sadłowska-Sałęga, A.; Radoń, J. Feasibility and limitation of calculative determination of hygrothermal conditions in historical buildings: Case study of st. Martin church in Wiśniowa. *Build. Environ.* **2020**, *186*, 107361. [CrossRef]
43. Nawalany, G.; Sokołowsk, P.; Michalik, M. Analysis of the Operation of an Unheated Wooden Church to the Shaping of Thermal and Humidity Conditions Using the Numerical Method. *Energies* **2021**, *14*, 5200. [CrossRef]
44. Sobczyk, J. Weryfikacja Metod Analizy Mikroklimatu Historycznych Budynków Muzealnych (Ang. Verification of Methods of Microclimate Analysis of Historical Museum Buildings). Ph.D. Dissertation, University of Agriculture in Kraków, Kraków, Poland, 2024.
45. Sadłowska-Sałęga, A.; Sobczyk, J.; del Hoyo-Meléndez, J.M.; Wąs, K.; Radoń, J. Preservation strategy and optimization of the microclimate management system for the Chapel of the Holy Trinity in Lublin. In Proceedings of the International Conference of Energy Efficiency in Historic Buildings (EEHB2018), Visby, Sweden, 26–27 September 2018.
46. Winkler, M.; Antretter, F.; Radoń, J. Critical discussion of a shading calculation method for low energy building and passive house design. *Energy Procedia* **2017**, *137*, 33–38. [CrossRef]
47. Wikimedia Commons. UlicaBracka-WidokNaPółnoc-POL, Kraków.jpg by Mach240390. Available online: https://commons.wikimedia.org/wiki/File:UlicaBracka-WidokNaP%C3%B3%C5%82noc-POL,_Krak%C3%B3w.jpg (accessed on 16 November 2024).
48. Repository of Building Simulation Climate Data. Available online: https://climate.onebuilding.org/ (accessed on 11 November 2024).
49. *EN 16798-1:2019*; Energy Performance of Buildings—Ventilation for Buildings, Part 1: Indoor Environmental Input Parameters for Design and Assessment of Energy Performance of Buildings Addressing Indoor Air Quality, Thermal Environment, Lighting and Acoustic. European Committee for Standardization: Brussels, Belgium, 2019.
50. Consequences of Climate Change. Available online: https://climate.ec.europa.eu/climate-change/consequences-climate-change_en (accessed on 11 November 2024).
51. Climate Change Indicators: Heat Waves. Available online: https://www.epa.gov/climate-indicators/climate-change-indicators-heat-waves (accessed on 11 November 2024).
52. *Extreme Weather Events in Europe: Preparing for Climate Change Adaptation*; Norwegian Meteorological Institute: Oslo, Norway, 2013.
53. Vardoulakis, S.; Fisher, B.; Pericleous, K.; Gonzalez-Flesca, N. Modelling air quality in street canyons: A review. *Atmos. Environ.* **2003**, *37*, 155–182. [CrossRef]
54. Mangan, S.; Oral, G.; Kocagil, I. The impact of urban form on building energy and cost efficiency in temperate-humid zones. *J. Build. Eng.* **2021**, *33*, 101626. [CrossRef]
55. Zielonko-Jung, K. Kształtowanie budynków energooszczędnych w przestrzeniach miejskich. In *Budownictwo Energooszczędne w Polsce—Stan i Perspektywy (Energy-Efficient Construction in Poland—Status and Prospects)*; Wesołowska, M., Podhorecki, A., Eds.; Wydawnictwa Uczelniane Uniwersytetu Technologiczno-Przyrodniczego w Bydgoszczy: Bydgoszcz, Poland, 2015; pp. 107–116.
56. Mao, C.; Baltazar, J.; Haberl, J. Comparison of ASHRAE peak cooling load calculation methods. *Sci. Technol. Built Environ.* **2018**, *25*, 189–208. [CrossRef]
57. Mao, C.; Baltazar, J.C.; Haberl, J.S. Literature review of building peak cooling load methods in the United States. *Sci. Technol. Built Environ.* **2017**, *24*, 228–237. [CrossRef]
58. Malicki, M. *Wentylacja i Klimatyzacja*; PWN: Warsaw, Poland, 1980.
59. Pełech, A. Wentylacja i klimatyzacja. In *Podstawy*; Oficyna Wydawnicza Politechniki Wrocławskiej: Wrocław, Poland, 2013.
60. Recknagel, H.; Sprenger, E. *Recknagel Taschenbuch für Heizung- und Klimatechnik 92/93*; R. Oldenbourg Verlag GmbH: Munich, Germany, 1991.